A Power Electronics Unit to Drive Piezoelectric Actuators for Flying Microrobots

Mario Lok, Xuan Zhang, Elizabeth Farrell Helbling, Robert Wood, David Brooks, Gu-Yeon Wei
Harvard University, Cambridge, Massachusetts, 02138 USA

Abstract—**This paper describes a power electronics unit (PEU) for an insect-scale flapping-wing robot. Three power saving techniques used in the actuator driver of the PEU—envelope tracking, dynamic common mode, and charge sharing—reduce power consumption while retaining weight benefits of an inductor-less linear driver. A pair of actuator driver ICs energize four 15nF capacitor loads, which represent the piezoelectric actuators of a flapping-wing robot. The PEU consumes 290mW, which translates to 37% lower power compared to a design without these power saving techniques.**

Index Terms – **piezoelectric actuator driver, high voltage driver, capacitive loads, BCD, microrobot**

I. INTRODUCTION

Harvard's RoboBee (Fig. 1a) is a milligram-scale aerial robot that produces lift through flapping-wing locomotion driven by two bimorph piezoelectric (PZT) actuators [1]. The robot recently achieved hovering and maneuvering along three axes while tethered to a bench-top high-voltage signal generator that drives the actuators. For full autonomy, one of the most critical challenges is to design an energy-efficient power electronics unit (PEU) to drive the piezoelectric actuators with a 200-300V sinusoidal voltage at the mechanical resonant frequency of the robot (approximately 80Hz) off a 3.7V battery while adhering to the 100mg payload weight budget of the robot.

With this objective in mind, this paper presents the design of a PEU comprised of the following three main components: (1) a tapped-inductor boost convertor, (2) two actuator-driver power ICs, and (3) feedback control circuitry embedded within an SoC, as shown in Fig. 2. The boost converter generates a high voltage supply, VDDH, from a 3.7V battery. The power IC implements a pair of linear drivers that charge and discharge the capacitance associated with the PZT actuators. A set of pulse-frequency-modulated signals generated by the SoC controls the boost converter to generate VDDH and drive the power switches in the linear driver to produce the high-voltage sinusoidal waveforms. The linear driver outputs are sampled through voltage dividers, fed back to the SoC through ADCs, and compared against a digital reference computed within the SoC. The feedback circuit ensures that the excitation waveform tracks the equations implemented in the signal compute block. The PEU uses discrete components for the boost converter for higher efficiency, and employs an integrated design for the actuator driver to minimize the overall weight. The design of the SoC is fully described in [3].

This paper focuses on the actuator driver block within the PEU, and proposes three power saving features—envelope tracking, dynamic common mode, and charge sharing—in order to reduce power consumption compared to previous integrated designs.

(a) Picture of RoboBee

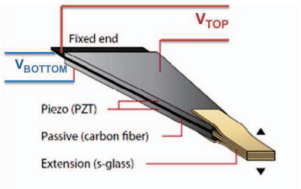

(b) Bimorph Actuator

Fig. 1: Harvard RoboBee is a milligram-scale flapping-wing robot with two bimorph actuators.

II. TOPOLOGY OPTIONS AND PRIOR DESIGNS

Before delving into the details of the power saving features, it is instructive to first review PZT actuator characteristics, available topology options, and previous actuator driver designs.

Each PZT bimorph actuator sandwiches two PZT layers about an insulating layer (Fig. 1b). The actuator deflects according to the differential voltage between the top and bottom layers (V_{TOP} -V_{BOTTOM}), wherein the two signals are 180 degrees out of phase. Actuator deflection directly translates to RoboBee wing stroke, which determines the thrust force produced by the flapping wings. Each actuator layer acts as a capacitive load to the driver circuits.

Depending on the polarization direction of the PZT layers, the PEU can energize the actuators via a simultaneous drive or an alternating drive topology—shown in Fig. 4 [4]. Both topologies rely on a boost converter to generate a high voltage supply VDDH from a 3.7V battery. For simultaneous drive, VDDH provides a constant high voltage bias (V_{BIAS}) across the series stack of the two PZT layers and a single sinusoidal signal drives the middle layer. In contrast, the alternating drive topology grounds the middle layer and drives the top and bottom PZT layers (connected in parallel) with a pair of out-of-phase sinusoids.

Given the stringent weight constraints of the RoboBee, the simultaneous drive topology may seem to be the obvious choice as it only requires one driver circuit per actuator. Assuming this drive topology, [1] achieved controlled flight via control signals for the left and right wings shown in Fig. 3, and these signals translate to torque along three axes. The sinusoidal waveforms for the actuators attached to the left and right wings (V_L, V_R) can be described by Eq. 1.

$$V_L, V_R = \frac{V_{Bias}}{2} + [(1-\mu)sin(\omega t) \pm \mu sin(2\omega t)] * \frac{(V_{amp} \pm V_{Roll})}{\gamma} + V_{Pitch} \quad (1)$$

978-1-4799-8682-8/15/$31.00 ©2015 IEEE

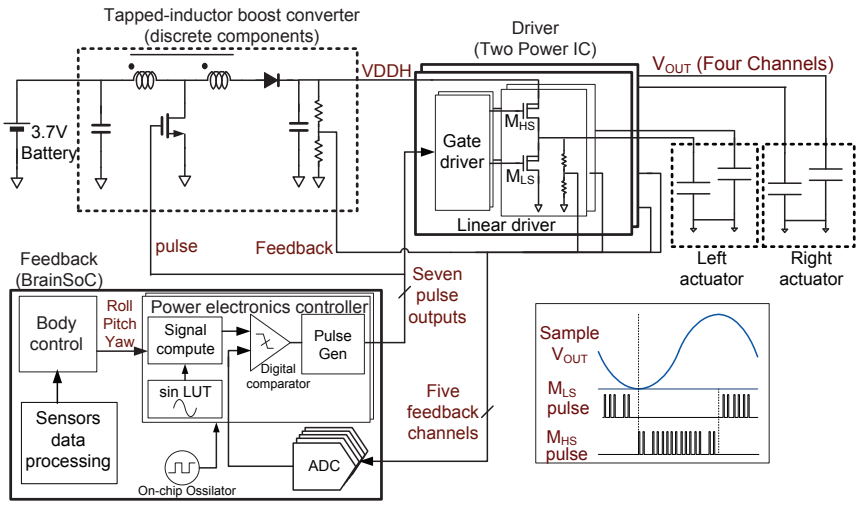

Fig. 2: A PEU design consists of two identical power ICs, a SoC and a off-chip boost converter.

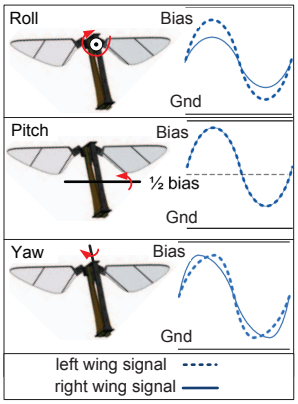

Fig. 3: Drive signals creates rotations in three axes.

Here, V_{amp} sets the nominal amplitude of the drive signal corresponding to average thrust. Asymmetric left and right wing stroke amplitudes (via V_{Roll}) leads to roll. Simultaneously shifting the DC bias (via V_{Pitch}) of the left and right sinusoids leads to pitch rotation due to a shift of the mean stroke angle relative to the robot's center of mass. Finally, adding a second harmonic to the sinusoid (via μ) leads to yaw rotation due to asymmetric up and down strokes. γ is a normalization constant corresponding to μ.

An early implementation of driver circuitry to energize PZT actuators for flapping-wing robots, described in [4], used discrete components to implement a switching amplifier design for simultaneous drive. A 15mg output inductor enabled energy recovery to reduce energy consumption by 50% compared to a push-pull linear driver. However, to add a second switching amplifier required by the dual-actuators would push the PEU beyond the weight budget. To reduce weight, a follow-on design integrated the switching amplifier onto a single chip using high-voltage DMOS transistors. However, the much higher parasitic C_{DS} capacitance of the transistors led to higher switching losses and results in only a 20% energy reduction [2]. For the RoboBee application, this 20% energy savings cannot overcome the 30mg weight penalty associated with two output inductors. Hence, the inductor-less, linear driver topology is preferred when the driver electronics are integrated into an IC. Moreover, given the low incremental cost of a transistor in an IC, the simultaneous drive topology may no longer be the best choice.

III. Power Saving Features

Building on prior work, this section proposes three energy-saving techniques, enabled by shifting to the alternating drive topology. These techniques compensate for the inefficiencies of an integrated linear driver while circumventing the weight penalty of output inductors. Although the alternating drive topology requires doubling the number of driver channels from two to four, the incremental size and weight increase for an integrated design is very small (3mg).

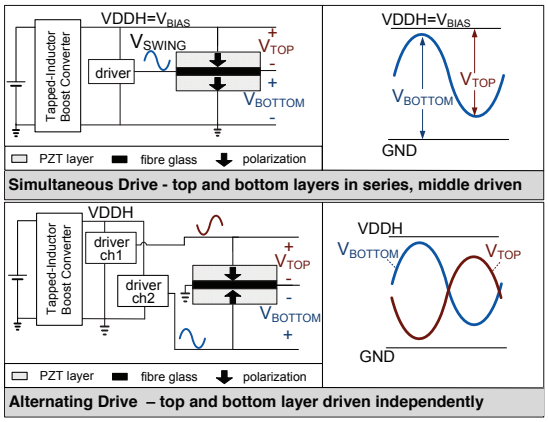

Fig. 4: There are two options to drive a bimorph PZT actuator. Simultaneous drive requires one driver connected to the middle layer. Alternating drive relies on two driver channels to generate out-of-phase sinusoids across the PZT layers with a grounded middle layer.

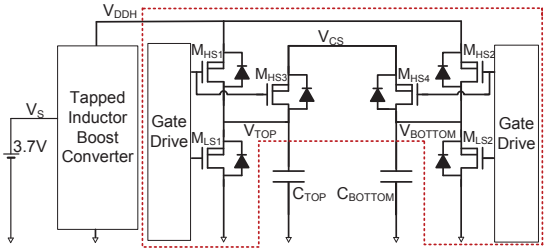

Fig. 5: The proposed actuator driver enables envelope tracking, dynamic common mode, and charge sharing to save power.

A. Envelope Tracking

Envelope tracking is a power-saving technique that dynamically modulates the supply voltage of the driver

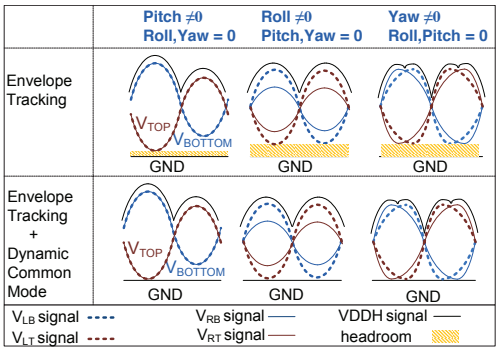

Fig. 6: Comparison between the roll, pitch, and yaw drive signals shows the adjustment to VBIAS and the common mode voltage while keeping differential voltage consistent for the simultaneous drive configuration.

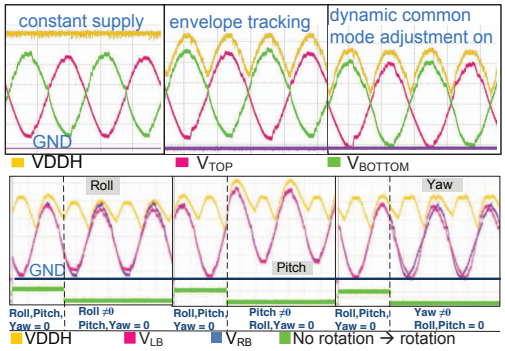

Fig. 7: Top row of oscilloscope waveforms of VDDH and top and bottom PZT drive signals demonstrate envelope tracking and dynamic common mode. Bottom row shows left and right driver waveforms for non-zero roll, pitch, and yaw rotation.

circuit to the minimum required to reliably generate its time-varying output signal [5]. Recall that the simultaneous drive topology requires a constant high voltage V_{BIAS}, which ensures that the voltage signals across the top and bottom PZT layers are always 180 degrees out of phase. In contrast, the alternating drive topology relies on two separate drivers to energize the two parallel PZT layers independently. Since this topology does not require a constant high voltage bias, there is an opportunity to dynamically reduce VDDH while reliably generating the desired output sinusoids across the two PZT layers, as shown in Fig. 6. The controller for the boost converter monitors output waveform requirements and appropriately sets VDDH. The control equations for the four output channels to the top and bottom layers of left and right actuators are given by Eqs. 2 and 3. The envelope tracking relationship between the output channels and VDDH is given by Eq. 4.

$$V_{LT}, V_{RT} = \frac{V_{Bias}}{2} - [(1-\mu)sin(\omega t) \pm \mu sin(2\omega t)] * \frac{(V_{amp} \pm V_{Roll})}{\gamma} - V_{Pitch} \quad (2)$$

$$V_{LB}, V_{RB} = \frac{V_{Bias}}{2} + [(1-\mu)sin(\omega t) \pm \mu sin(2\omega t)] * \frac{(V_{amp} \pm V_{Roll})}{\gamma} + V_{Pitch} \quad (3)$$

$$V_{DDH} = max\{V_{LT}, V_{LB}, V_{RT}, V_{RB}\} + V_{Margin} \quad (4)$$

Envelope tracking reduces power consumption in two ways. First, it minimizes the voltage level of VDDH from which current is drawn to charge the capacitive actuator loads. Secondly, the boost converter's efficiency improves when supplying power at a lower output voltage.

B. Dynamic Common Mode

The second power-saving feature involves dynamically adjusting the common mode voltage of the drive signals with respect to the roll, pitch and yaw control, minimizing voltage headroom and thereby reducing energy. Recall that each of the two actuators deflect according to the differential signal, $V_{TOP} - V_{BOTTOM}$, while the common mode signal $\frac{V_{TOP}+V_{BOTTOM}}{2}$ does not contribute to actuator motion. Lowering common mode voltage levels reduces the power consumed to generate theV_{TOP} and V_{BOTTOM} signals as it leads to simultaneous reduction in the DC level signals V_{TOP} and V_{BOTTOM}. The minimum common mode level is constrained by the requirement that both V_{TOP} and V_{BOTTOM} need to remain positive to keep the PZT layers in contraction mode for reliability reasons.

Moreover, since the excitation signals V_{TOP} and V_{BOTTOM} depend on roll, pitch and yaw inputs from the body control of the robot, the minimum allowable common mode voltage also changes with the control inputs. Thus, to maximize power reduction, the PEU design must track the minimum common mode voltage dynamically with respect to the control inputs. The resulting dynamic relationship is given by Eq. 5.

$$V_{CM} = \frac{(V_{amp} + |V_{Roll}|)}{2} + |V_{Pitch}| \quad (5)$$

Correspondingly, we need to modify Eqs. 2 and 3 in the signal compute block in the SoC to support this dynamic common mode adjustment scheme. For example, the modified equation with dynamic common mode for Eq. 2 is given by Eq. 6.

$$V_{LT}, V_{RT} = \frac{(V_{amp} + |V_{Roll}|)}{2} + |V_{Pitch}| - [(1-\mu)sin(\omega t) \pm \mu sin(2\omega t)] * \frac{(V_{amp} \pm V_{Roll})}{\gamma} - V_{Pitch} \quad (6)$$

Fig. 6 illustrates the benefits of dynamic common mode adjustment for the alternating drive scenario. Dynamic common mode further reduces the envelope voltage by reducing voltage headroom, as labelled in the figure.

C. Charge Sharing

Charge sharing is the third power-saving technique, which seeks to reduce power by moving charge between two parallel actuator capacitors [6]. Implementation of this charge sharing concept is shown in Fig. 5, controlled by switches M_{HS3} and M_{HS4}. Since the sinusoidal waveforms across the two PZT layers in an actuator are always 180 degrees out of phase, charge sharing is possible for half of each sinusoidal cycle. When M_{HS3} turns on, this design

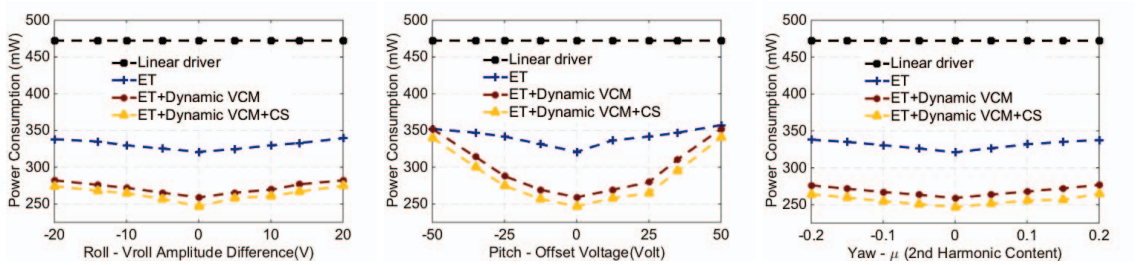

Fig. 8: The total power consumption changes depending on roll, pitch and yaw commands.

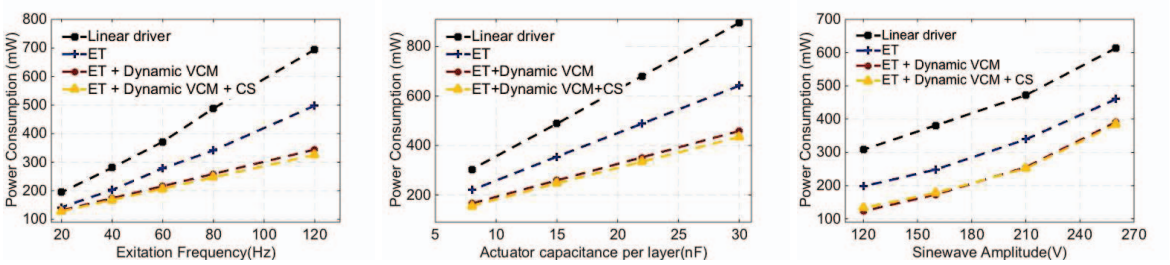

Fig. 9: Total power consumption scale with excitation frequency, actuator capacitance, and sinusoidal drive signal amplitude.

allows current to flow from C_{BOTTOM} to C_{TOP} via M_{HS3} and body diode of M_{HS4}. Unfortunately, parasitic PNP transistors, connected to the body diodes of these charge sharing switches, turn on and draw away most of the charge to the substrate rather than charging up the other capacitor. Thus, this feature was much less effective than originally simulated. While the problematic parasitic transistor comes from the shared substrate in the bulk DMOS process used, future high-voltage silicon-on-insulator (SOI) processes would not have this problem.

IV. EXPERIMENTAL RESULTS

To evaluate the power saving features described above, we built and tested a PEU with an off-chip boost converter, two power ICs, and an SoC to drive four 15nF capacitors with 80Hz 200V peak-to-peak excitation waveforms, where the four capacitors represent two piezoelectric actuators.

Fig. 7 verifies proper operation of the envelope tracking and dynamic common mode adjustment features for two drive channels of a single actuator with zero roll, pitch, and yaw settings. The bottom scope capture shows left and right drive signals responding to changes in flight control input on the falling edge of an indicator signal. This validates that the driver and the controller can appropriately drive the actuators for roll, pitch, and yaw rotation while utilizing envelope tracking and common mode adjustment.

Since roll, pitch, and yaw determine the drive signal swings and the envelope voltage, Fig. 8 plots the measured power consumption of the entire PEU across the full range of roll, pitch, and yaw settings. With envelope tracking and common mode adjustment turned on, up to 48% power reduction is achieved over the original linear driver. Based on the roll, pitch, and yaw data collected from a realistic flight test, the average power consumed by the PEU is 290mW, 37% less than the power consumed by a PEU that uses linear drivers.

Fig. 9 plots the total power consumption of the proposed PEU across a range of excitation frequencies, capacitor loads, and output sine wave amplitudes. These results verify that the proposed PEU can support a wide range of applications with different output power and actuator characteristics.

Lastly, Fig. 10 presents a die photo of the power IC that integrates two high-voltage linear drivers.

ACKNOWLEDGMENTS

Authors thank TSMC's university shuttle program for chip fabrication. This work was supported in part by NSF (IIS-0926148 and CCF-1218298) and DARPA (HR0011-13-C-0022).

REFERENCES

[1] Ma, K.Y., et al. "Controlled flight of a biologically inspired, insect-scale robot." *Science*, 2013.
[2] Lok, M., et al. "Design and analysis of an integrated driver for piezoelectric actuators." *ECCE*, 2013.
[3] Zhang, X., et al. "A Multi-Chip System Optimized for Insect-Scale Flapping-Wing Robots," *Symp. VLSI Circuits*, 2015.
[4] Karpelson, M., et al. "Milligram-scale high-voltage power electronics for piezoelectric microrobots," *Int'l Conf. Robotics and Automation*, 2009.
[5] Wang, F., et al. "Envelope Tracking Power Amplifier with Pre-distortion for WLAN 802.11g," *IEEE MTT-S*, 2004.
[6] McCreary, J., et al. "All-MOS charge redistribution analog-to-digital conversion techniques." *JSSC*, 1975.

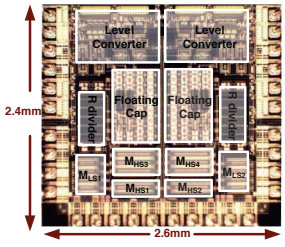

Fig. 10: Chip photograph for the power IC.